

Mass spectrometric studies on the decomposition of trialkylgallium on GaAs surfaces

Yoshimasa Ohki* and Yuji Hiratanit

Optoelectronics Technology Research Laboratory, 5-5 Tohkodai, Tsukuba, Ibaraki 300-26, Japan

The thermal decomposition of trimethylgallium $[(CH_3)_3Ga]$ and triethylgallium $[(C_2H_5)_3Ga]$ on gallium arsenide (GaAs) surfaces was studied under an ultra-high vacuum using mass spectrometry. It was observed that the decomposition process of $(CH_3)_3Ga$ and $(C_2H_5)_3Ga$ depends on the arsenic coverage of the substrate surface. On a (100)-oriented surface, increasing the arsenic coverage basically enhances the decomposition of $(CH_3)_3Ga$ and $(C_2H_5)_3Ga$ to gallium atoms above 350 and 300 °C, respectively. The decomposition of $(CH_3)_3Ga$ proceeds by emitting CH_3 radicals. On a surface with low arsenic coverage, the decomposition of $(CH_3)_3Ga$ is imperfect and fewer than three methyl groups of alkylgallium are desorbed. On a (111)B-oriented surface, however, an increase in the surface arsenic coverage suppresses the decomposition of alkylgallium, which is different from the case for a (100) surface.

Keywords: Gallium arsenide, trimethylgallium, triethylgallium, mass spectrometry, thermal decomposition, metal-organic molecular beam epitaxy (MOMBE), growth mechanism, surface reconstruction

1 INTRODUCTION

The epitaxial growth of compound semiconductors using metal-organics as source materials is widely applied to the fabrication of both electronic and optoelectronic devices. For example, laser diodes or high-electron mobility transistors are produced in practice by metal-organic vapor-

phase epitaxy (MOVPE) as well as by molecular beam epitaxy (MBE). Research in this field has included fabrication studies as well as investigation of the quantum size [less than 500 Å (50 nm) in size] of heterostructures or mesoscopic structure. These materials have attracted much attention since such structures are expected to open up a new field in basic research¹ while improving device performance drastically.² Fabrication of very fine structures is, therefore, very important and useful for both research and industrial fields. To fabricate such small structures, it is necessary to understand the growth mechanism and to control the growth processes precisely.

Metal-organic molecular beam epitaxy (MOMBE) involves a combination of MBE and MOVPE,³ and some advantages over these two epitaxy techniques, especially concerning the fabrication of fine structures: (1) the growth reaction involves chemical nature and takes place only on substrate surfaces, (there are no vapor-phase reactions); (2) surface reactions can be controlled by external excitation such as energetic electrons or a photon beam; (3) chemical species which can modify the surface reaction can be introduced; and (4) since growth is carried out in a high vacuum, many real-time monitoring and *in situ* analysis techniques can be used both to study and to control the epitaxial growth.

We have been studying the thermal decomposition of trialkylgallium on gallium arsenide (GaAs) surfaces using mass spectrometry,^{4,5} since this technique can detect chemical species related to the growth reaction in MOMBE. Furthermore, a quadrupole mass spectrometer (QMS) can be used for the real-time monitoring method during MOMBE when a fairly high operating pressure (in our experiment $<2 \times 10^{-4}$ Pa) of the reactive gases is employed. It should be noted that electron spectroscopy, such as Auger electron and X-ray photoelectron spectroscopy, cannot be used in ambient reactive gas.

* Present address: Semiconductor Research Center, Matsushita Electric Industrial Co. Ltd, 3-10-1 Higashimita, Tama-ku, Kawasaki 214, Japan.

† Present address: Yokohama R&D Laboratories, The Furukawa Electronic Co. Ltd, 2-4-3 Okano, Nishi-ku, Yokohama 220, Japan.

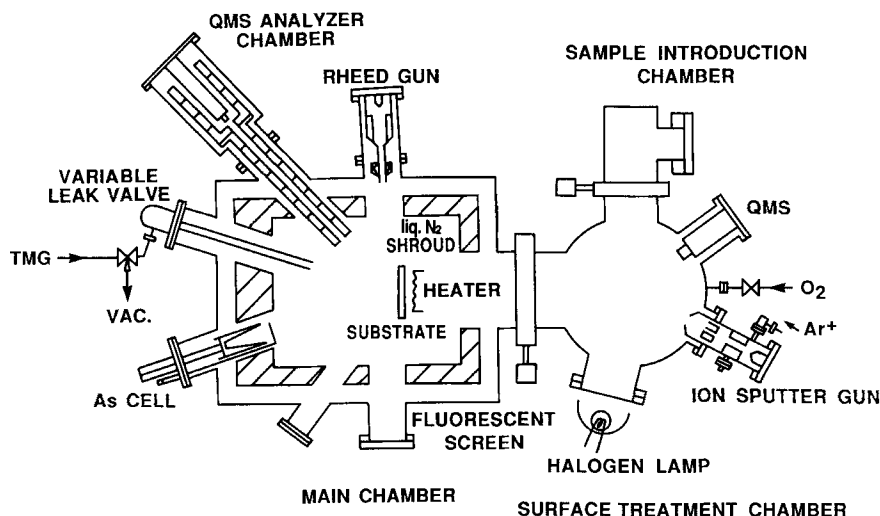


Figure 1 Schematic illustration of the MOMBE system used in this study. TMG, $(\text{CH}_3)_3\text{Ga}$ (trimethylgallium).

In this paper we present the results of mass spectrometric measurements of species desorbed or reflected from a substrate surface as a function of the surface-preparation method, substrate temperature and exposing flux density. The results obtained were interpreted in terms of the effects of the substrate surface arsenic coverage, or of the As_4 flux supplied density, on the thermal decomposition process of trimethylgallium $[(\text{CH}_3)_3\text{Ga}]$ and triethylgallium $[\text{C}_2\text{H}_5)_3\text{Ga}]$ on GaAs surfaces.

2 EXPERIMENTAL

2.1 Apparatus

Measurements were carried out in a specially designed ultra-high-vacuum MOMBE system (Fig. 1). This MOMBE system comprises four chambers: a sample introduction chamber, a surface treatment chamber, a main chamber and a QMS analyzer chamber. The sample introduction chamber is evacuated by a turbo-molecular pump (TMP) down to 2×10^{-5} Pa. The surface treatment chamber is evacuated by a TMP and an ion pump (IP) to less than 5×10^{-8} Pa. This chamber is connected to the main chamber as well as to the sample introduction chamber (through which samples are introduced into the main chamber). The main purpose of this chamber involves the formation of a thin surface-oxidized layer of GaAs, which is used as a mask material for selective-area epitaxy.⁶ An oxygen (O_2) gas line

with a leak valve is attached to this chamber. From this gas line, high-purity O_2 gas is introduced when oxidizing a substrate surface. A GaAs wafer in the chamber is irradiated with light from a halogen lamp through a view port under an O_2 atmosphere to form a thin GaAs oxide layer. This chamber is also equipped with an Ar^+ ion-sputtering gun which can be used to remove the surface GaAs oxide layer locally.

The main chamber, evacuated by a TMP and an IP with a base pressure less than 5×10^{-8} Pa, is used for substrate surface cleaning, epitaxial growth and measurements. The operating pressure depends on the experimental conditions and is typically $(1-50) \times 10^{-6}$ Pa. In order to supply source materials, this chamber is provided with both solid source effusion cells and gas nozzles. An effusion cell containing solid arsenic is used for generating an As_4 flux, the density of which is changed by varying the cell temperature. The arsenic cell and its shutter is recessed into the source shroud so as to reduce the arsenic background pressure to less than 5×10^{-7} Pa when the arsenic-cell shutter is closed. Gas nozzles are used to introduce MOs into the main chamber and to expose the substrate surface to MOs. Pure MO vapor evaporated from a stainless-steel bottle is used without any carrier gas in order to avoid any effect of the carrier gas on the measured results. The supply rate of each MO is controlled by a variable-leak valve. The vent/supply of MO is performed by a gas manifold system, and the vent line is evacuated by a TMP. The main chamber is equipped with a conventional reflection high-

energy electron diffraction (RHEED) system, which is used to monitor the surface reconstruction and intensity of a diffracted spot. An electron beam with an energy of 20 keV[†] is incident mainly on the [110] azimuth for both (100) and (111)B surfaces.

The QMS analyzer chamber is attached to the main chamber and is evacuated differentially by an IP to less than 4×10^{-8} Pa. This chamber is provided with a liquid-nitrogen circulating shroud as well as an aperture assembly in which a QMS analyzer is installed. The cold aperture limits the line-of-sight area of the QMS ionizer at the substrate position to less than 3 cm in diameter. Hence, if a wafer that is 5 cm in diameter is used, the signal of the QMS is mainly due to the species either reflected or desorbed from the substrate surface. The QMS system used in this study could detect species of mass number up to about 360, and was used in a mass spectrum mode and in a multiple ion selector (MIS) mode.

The temperature of the substrate surface was routinely measured by an optical pyrometer which was calibrated by measuring the surface temperature of a dummy wafer with a thin thermocouple attached to the substrate surface, the top of the thermocouple was placed in a small piece of indium located on the dummy wafer surface.

2.2 Substrate preparation

Semi-insulating (SI) and Si-doped n-type GaAs with (100)- and (111)B-oriented wafers (both 5 cm in diameter) were used as substrates. Since no difference in the results between SI and n-type substrates was observed in this experiment, we neglect these two conduction types in the remainder of this paper. A fused quartz plate was also used for reference measurements.

The substrate was first degreased using organic solvents, and etched in a sulfuric acid etchant to remove both surface contamination and any damaged layer; it was then rinsed in flowing deionized water. After being spin-dried, the substrate was mounted on a molybdenum sample holder with high-purity indium in air. The substrate on the molybdenum sample holder was introduced into the main chamber via the sample introduction chamber and the surface treatment chamber. The substrate was heated to 630 °C in an As₄ flux in order to evaporate the oxidized

surface layer. When the oxide was evaporated, an increase in the QMS signal for mass numbers of 69 and 71 (both Ga) as well as 154, 156 and 158 (we assign as Ga₂O) was observed. The RHEED pattern changed from a weak specular spot in a diffused background to a somewhat-diffused 2×4 -like pattern for a (100)-oriented and a 2×2 structure for a (111)B-oriented substrate after evaporation of the oxidized surface layer.

The starting substrate surface was prepared in a slightly different way for each measurement, as described in other parts of this paper.

2.3 Measurement method

The QMS analyzer used in this study can be operated with an ionization energy ranging from 20 to 100 eV. The electron impact ionization in the QMS analyzer resulted in the decomposition of trimethylgallium [(CH₃)₃Ga] into fragment species. Since the signal of (CH₃)₃Ga⁺ was very small to detect its intensity variation, signals of (CH₃)₂Ga⁺, (CH₃)Ga⁺ and Ga⁺ (and hydrocarbons) were measured. The ratios between the signals of the fragment species, the cracking coefficients, depended slightly on the ionization energy. For example, Ga⁺/(CH₃)₂Ga⁺ decreased by about 10 % in the low ionization energy region. The maximum signal intensity was obtained at around 70–80 eV and decreased to 30 % of the maximum intensity in the low ionization energy region. We therefore used an ionization energy of 70 eV to obtain a sufficient signal intensity throughout this study. The signal intensities of the gallium-containing species were mainly measured since they contain information concerning the decomposition of MOs on the substrate surface. It is well known that the signal intensity ratios between fragment species are uniquely determined for a compound, independently of both its concentration and flux density. Hence, the signal intensity ratios were used to assign the incident species to the QMS analyzer.

3 RESULTS AND DISCUSSION

3.1 Decomposition of MOs on a (100) 2×4 surface

The GaAs (100) surface is widely used as a substrate for MOMBE as well as for MBE or MOVPE, since high-quality epitaxial layers can

[†] 1 eV = 96.4853 kJ mol⁻¹.

be easily grown on surfaces of this type. Reconstruction of the surface orientation has been extensively studied using low-energy electron diffraction,⁷ RHEED,⁸ and, recently, scanning tunneling microscopy (STM).⁹ Even though many surface-reconstructed structures have been reported, a 2×4 As-stabilized structure is stable and has been commonly used as the surface structure during growth by MBE or MOMBE. Atomic layer epitaxy (ALE), which is the ultimate epitaxy technique using layer-by-layer growth with a self-limiting mechanism, has also been reported regarding this surface.¹⁰ A small number of reports have been concerned with *in situ* mass spectrometric measurements of the reaction between surfaces with the 2×4 structure and MOs;¹¹ the effects of arsenic-source flux on the decomposition of MOs has not been mentioned.

The starting 2×4 structure for this measurement was prepared for each measurement by growing about 20 MLs of GaAs at 570°C by simultaneously supplying $(\text{CH}_3)_3\text{Ga}$ and As_4 , followed by annealing for 10 min. The substrate was cooled to a specified temperature for measurement and then exposed to $(\text{CH}_3)_3\text{Ga}$ without an As_4 flux. The signal intensities of the gallium-containing species either desorbed or reflected from the substrate surface were measured while a surface with the 2×4 structure was exposed to $(\text{CH}_3)_3\text{Ga}$ for several minutes. The beam equivalent $(\text{CH}_3)_3\text{Ga}$ pressure was fixed at 6×10^{-6} Pa. Figure 2 shows the time variation of the Ga^+ signal intensity measured at three typical temperatures, which is similar to that in the previous report⁵ but the variation of signals is more clearly observed. It was observed that a smaller steady-state signal intensity results at elevated substrate temperatures, as discussed in Section 3.2. In this section we discuss the time variation of the signal intensity during the initial stage of $(\text{CH}_3)_3\text{Ga}$ exposure.

When a substrate at 300°C was exposed to $(\text{CH}_3)_3\text{Ga}$ [curve (a)], the Ga^+ signal increased sharply to a steady-state value. The RHEED pattern remained unchanged at (and below) this temperature. This means that incident $(\text{CH}_3)_3\text{Ga}$ molecules were reflected from the surface without any thermal decomposition. When exposure to $(\text{CH}_3)_3\text{Ga}$ was carried out at the substrate temperature of 450°C [curve (b)], the Ga^+ signal gradually increased to its steady-state value. The RHEED pattern at first changed from the 2×4 structure to a 1×1 or a diffused 1×2 structure.¹¹ This structure remained if the $(\text{CH}_3)_3\text{Ga}$ exposure

was suspended for several minutes. Upon further exposure to $(\text{CH}_3)_3\text{Ga}$ the diffraction streaks faded away and the specular spot intensity was enhanced markedly. The specular spot intensity became saturated when the Ga^+ signal was saturated. The diffused 1×2 structure was observed only within a narrow temperature range (at around 450°C). These observations suggest that some chemical reaction took place between $(\text{CH}_3)_3\text{Ga}$ molecules and the GaAs surface. At a substrate temperature of 550°C [curve (c)], the time variation of the Ga^+ signal showed a step-wise increase to its steady-state value. The RHEED intensity varied drastically during the step period in the Ga^+ signal. Although the reason is not clear, the RHEED intensity of a $(0, \frac{1}{4})$ streak varied in the reverse phase to the variation of a $(0, 0)$ streak (the specular spot). The RHEED pattern changed from the 2×4 structure to a 1×6 structure, which is considered to be a gallium-stabilized surface.¹²

The step in the time variation of the Ga^+ signal [as well as that of the CH_3Ga^+ and $(\text{CH}_3)_2\text{Ga}^+$ signal] indicates that the decomposition rate of

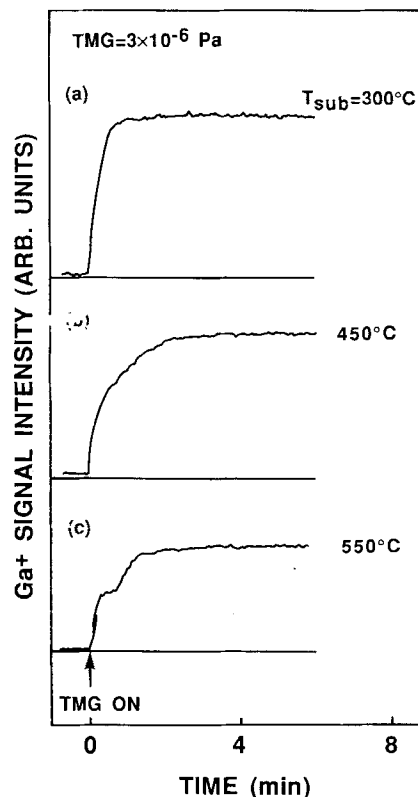


Figure 2 Time variation of the Ga^+ signal intensity at three typical substrate temperatures.

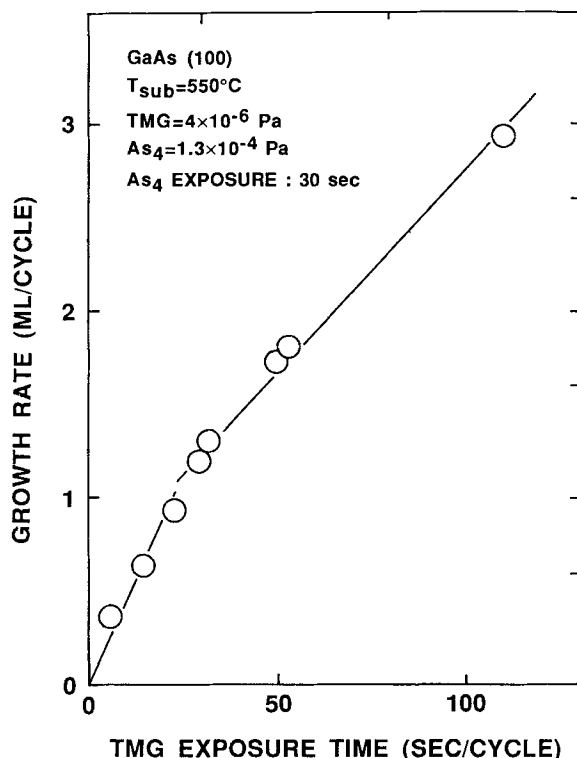


Figure 3 Growth rate versus the TMG exposure time for alternating source supply mode growth at 550 °C.

$(\text{CH}_3)_3\text{Ga}$ is faster on an arsenic-stabilized surface than on a gallium-stabilized surface, since the increase in the Ga^+ signal was due to an increase in either desorbed or reflected alkylgallium. To confirm this, the growth rate of the epitaxial layers was measured using an alternating source supply mode with various $(\text{CH}_3)_3\text{Ga}$ supply times. Figure 3 shows the growth thickness (in monolayer (ML) units) versus the $(\text{CH}_3)_3\text{Ga}$ exposure time for one cycle at a substrate temperature of 550 °C. The $(\text{CH}_3)_3\text{Ga}$ exposure time required to grow the first 1 ML was shorter than that required to grow the second and following MLs. The gradient of this curve showed that the growth rate of the first 1 ML was about twice that of the second and following MLs. Hence, a stepwise variation in the Ga^+ signal observed at 550 °C was due to a difference in the decomposition rate of $(\text{CH}_3)_3\text{Ga}$ between the 2×4 arsenic-stabilized and the 1×6 gallium-stabilized GaAs (100) surfaces; the decomposition rate of $(\text{CH}_3)_3\text{Ga}$ on the 2×4 arsenic-stabilized surface is twice as fast as that on the gallium-stabilized surface at 550 °C.⁵

If $(\text{C}_2\text{H}_5)_3\text{Ga}$ was used instead of $(\text{CH}_3)_3\text{Ga}$ in the same measurement, the signals of the gallium-

containing species gradually tended to saturation value above 300 °C (this onset temperature of decomposition was about 50 °C lower than that of $(\text{CH}_3)_3\text{Ga}$); still the steplike behavior of the Ga^+ signal was absent at any temperature ranging from room temperature to 580 °C.

3.2 Effects of As_4 flux on the decomposition of $(\text{CH}_3)_3\text{Ga}$

In the previous section, the decomposition of $(\text{CH}_3)_3\text{Ga}$ during the initial stage of $(\text{CH}_3)_3\text{Ga}$ exposure on an arsenic-stabilized surface was described. The decomposition rate of $(\text{CH}_3)_3\text{Ga}$ largely depends not only on the substrate temperature, but also on the surface reconstruction structure. In this section, the effect of the As_4 flux density on the decomposition pathway is discussed.^{13,14}

Figure 4 shows the temperature dependence of the steady-state values of the gallium-containing species measured under two extreme As_4 flux conditions. Figure 4(a) shows the results measured under an As_4 flux of 2×10^{-4} Pa. The signal intensity of each gallium-containing species varies with the substrate temperature in a similar manner. They dropped rapidly above 350 °C to about one-half of their initial values and had a minimum at about 500 °C, and then increased to a small maximum at around 550 °C. The diminution of the maximum in the Ga^+ signal by a decrease in the As_4 flux density accounts for the reported arsenic source pressure dependence on the growth rate.¹⁵ The small maximum at around 550 °C in the temperature dependence of the gallium-containing species became less pronounced upon decreasing the As_4 flux density. Such a substrate temperature dependence of the desorbed gallium-containing species was the reverse of that of the growth rate of GaAs by MOMBE.^{11,16} Measurements of the arsenic species showed that an increase in the substrate temperature resulted in a monotonic decrease in the intensities of As^+ , As_3^+ , and As_4^+ ; the substrate temperature dependence of As_2^+ has a minimum at around 500 °C, which is coincident with the minimum of the signal of the gallium-containing species.¹³

Figure 4(b) shows the signal intensities of the gallium-containing species versus the substrate temperature measured in the absence of As_4 flux. The signal intensities of both Ga^+ and $(\text{CH}_3)_2\text{Ga}^+$ decrease to about one-half of their initial values when the substrate temperature exceeds 350 °C,

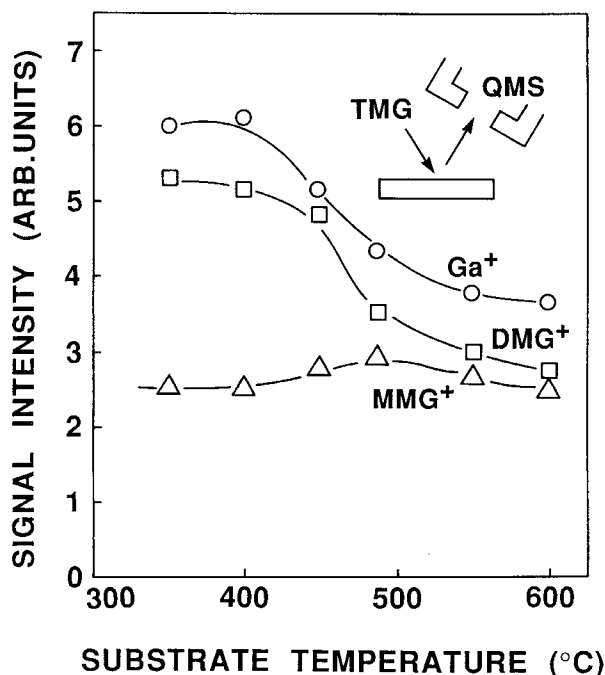
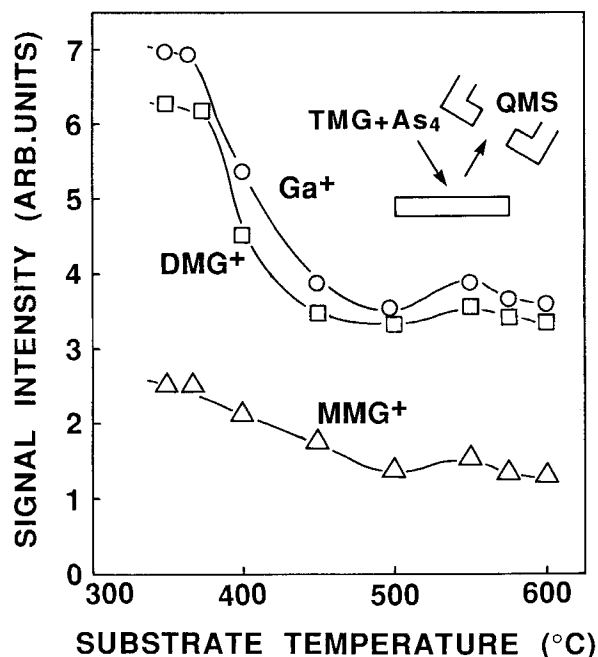


Figure 4 Steady-state signal intensity of gallium-containing species versus substrate temperature: (a) under an As_4 flux of 2×10^{-4} Pa; (b) in the absence of an As_4 flux. TMG, $(\text{CH}_3)_3\text{Ga}$; DMG $^+$, $(\text{CH}_3)_2\text{Ga}^+$; MMG $^+$, CH_3Ga^+ .

and show no hump at around 550°C (which was observed under sufficient As_4 flux). The drop in the signal intensity of $(\text{CH}_3)_2\text{Ga}^+$ is steeper than that of Ga^+ . Furthermore, the most prominent point of this figure is that the signal intensity of CH_3Ga^+ is almost independent of the substrate temperature, or has a small, and broad, maximum at around 500°C . This temperature dependence of the CH_3Ga^+ signal differs from those of Ga^+ and $(\text{CH}_3)_2\text{Ga}^+$ under an As_4 flux-free condition, and also differs from those of the gallium-containing species observed under a sufficient As_4 flux condition.

In order to assign the species desorbed from the substrate, the signal intensity ratio between fragments was studied. Figure 5(a) shows the signal intensity ratios against the substrate temperature obtained under similar conditions to those shown in Fig. 4(a); $(\text{CH}_3)_3\text{Ga}$ was therefore supplied simultaneously with the As_4 flux. The signal intensity ratios are almost independent of the substrate temperature, indicating that the desorbed species are the same at substrate temperatures ranging from 300 to 600°C . $(\text{CH}_3)_3\text{Ga}$ does not decompose effectively on a substrate surface below 350°C . These two facts indicate that $(\text{CH}_3)_3\text{Ga}$ molecules impinging on the surface at 300 – 600°C were desorbed without any accompanying decomposition. The signal intensity ratios shown in this figure represent the cracking coefficients of $(\text{CH}_3)_3\text{Ga}$. In other words, desorbed gallium-containing species are mainly undecomposed $(\text{CH}_3)_3\text{Ga}$ at least below 600°C under simultaneous supply of $(\text{CH}_3)_3\text{Ga}$ and As_4 . We call such a desorption process of TMG 'reflection' in this paper. A small increase in the signal intensity ratios in the high-temperature region may be caused by a small amount of desorbed alkylgallium with one or two methyl groups¹⁴ (described in the next paragraph).

Figure 5(b) shows the signal intensity ratios against the substrate temperature obtained in the absence of an As_4 flux. They increase markedly with an increase in the substrate temperature above 350°C . The increase in the signal intensity ratios of $\text{Ga}^+ / (\text{CH}_3)_2\text{Ga}$ and $\text{CH}_3\text{Ga}^+ / (\text{CH}_3)_2\text{Ga}$ indicates that alkylgallium with fewer methyl groups increases relative to that with more methyl groups. This means that some gallium-containing species other than $(\text{CH}_3)_3\text{Ga}$ were desorbed. The increase in the signal intensity ratio $\text{CH}_3\text{Ga}^+ / \text{Ga}^+$ means that the desorbed species were not gallium atoms but rather gallium with methyl groups. The desorption of gallium atoms from a GaAs surface

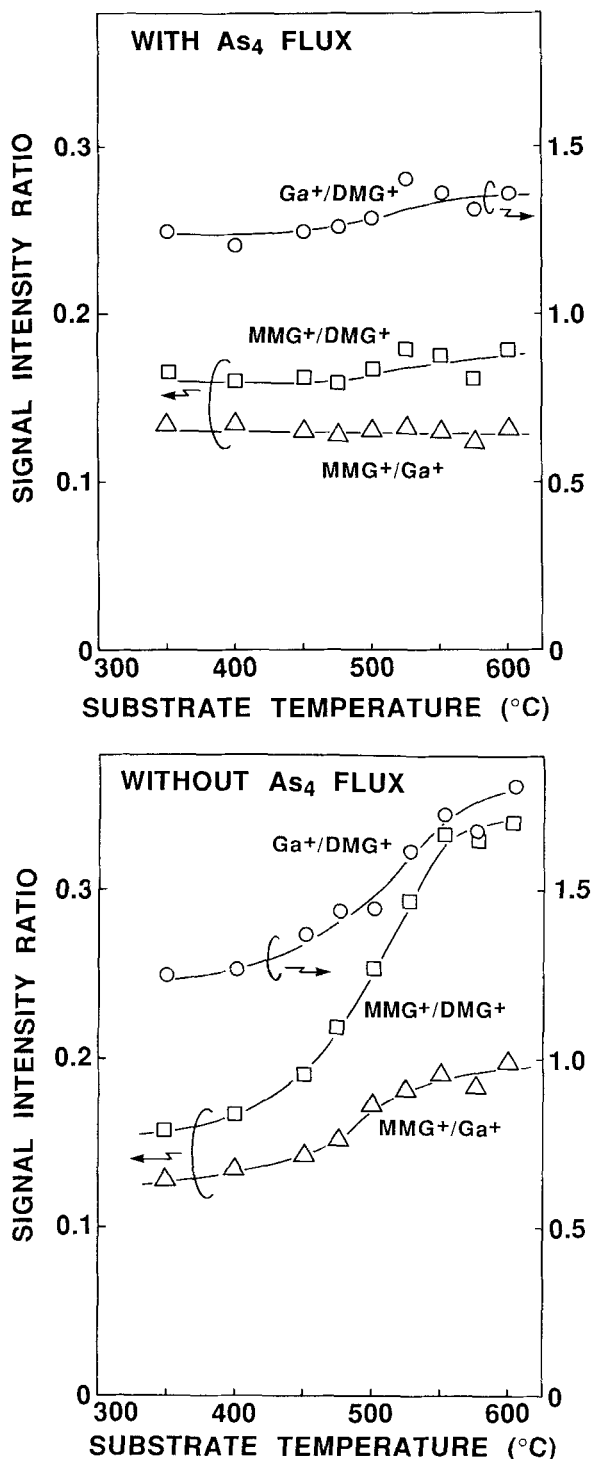


Figure 5 Signal intensity ratios [$\text{Ga}^+/(\text{CH}_3)_2\text{Ga}^+$, $\text{CH}_3\text{Ga}^+/(\text{CH}_3)_2\text{Ga}^+$, and $\text{CH}_3\text{Ga}^+/\text{Ga}^+$] versus the substrate temperature: (a) under an As_4 flux of 2×10^{-4} Pa; (b) in the absence of an As_4 flux. Abbreviations as in Fig. 4.

could be neglected, since the decomposition of GaAs was not severe below 600°C : hence, there was no contribution to the Ga^+ signal. We therefore conclude that some alkylgallium with fewer than three alkyl groups (mono- or di-methylgallium) was desorbed from the GaAs (100) surface when exposed to $(\text{CH}_3)_3\text{Ga}$ in the absence of an As_4 flux.

In order to study the decomposition mechanism, hydrocarbons CH_3^+ , CH_4^+ and C_2H_6^+ were also measured under the As_4 flux-free condition.³ The signal intensities of CH_3^+ and CH_4^+ have relatively high backgrounds in the apparatus used, even at low substrate temperatures, because of its continued previous use for experiments with $(\text{CH}_3)_3\text{Ga}$. In spite of such an unfavorable situation, the variation of the CH_3^+ and CH_4^+ signals with substrate temperature was observed by using the cold aperture. Figure 6 shows the substrate temperature dependence of both the CH_3^+ (open circles) and CH_4^+ (closed circles). Above 400°C , the signal intensity of CH_3^+ increased markedly, while that of CH_4^+ slightly decreased. This temperature is almost the same as that where the decrease in the signals of gallium-containing species were observed. Ethane

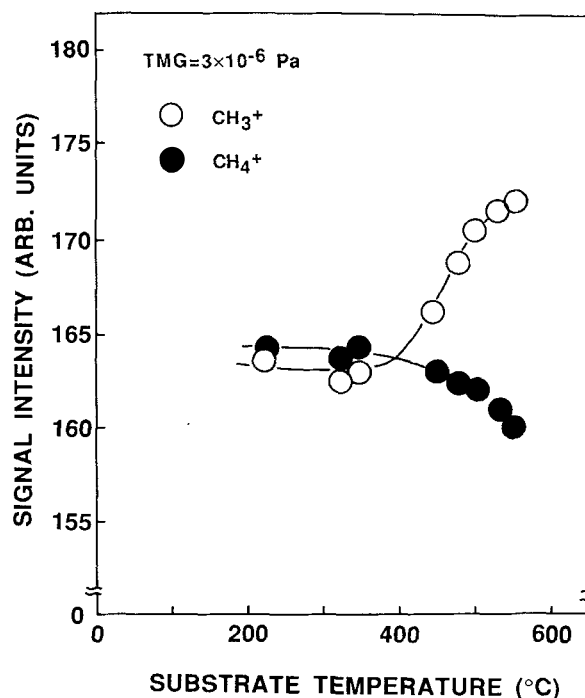


Figure 6 Signal intensity of CH_3^+ (○) and CH_4^+ (●) versus the substrate temperature. TMG, $(\text{CH}_3)_3\text{Ga}$.

($C_2H_6^+$), which is expected to be formed by dimerization of CH_3 , was observed only as a very small peak in the mass spectra both with and without exposure of the substrate to $(CH_3)_3Ga$. No temperature dependence of the $C_2H_6^+$ signal could be detected in our system below $550^\circ C$. This means that ethane is not the main reaction product of the thermal decomposition of $(CH_3)_3Ga$. Similar results were also obtained for the measurement with As_4 flux. These results indicate that, when decomposing, the TMG molecules impinging on the heated GaAs surface released CH_3 by breaking the Ga—C bond. The release of CH_3 from a GaAs surface was first reported by authors,⁴ and recently confirmed by modulation beam mass spectrometry¹⁷ and a temperature-programmed desorption¹⁸ study.

When a SiO_2 plate or GaAs with a thin oxidized surface layer was used as the substrate under similar measurements, increasing the substrate temperature to $550^\circ C$ induced a gradual decrease in the Ga^+ signal to 80 % of the intensity at $300^\circ C$. Furthermore, the signal intensity ratio between fragment species was independent of the temperature. These results indicate that the impinging $(CH_3)_3Ga$ was reflected on the surface of the SiO_2 plate as well as that of the oxide of GaAs. A gradual decrease in the Ga^+ signal could be understood as resulting from an increase in the translational velocity of $(CH_3)_3Ga$ molecules upon obtaining energy from the heated substrate. A smaller ionization probability in a QMS, and also a smaller signal, resulted when the velocity of molecule increased.

These results are summarized schematically in Fig. 7 in the form of decomposition pathways of $(CH_3)_3Ga$ both with and without an As_4 flux. When the substrate was exposed to $(CH_3)_3Ga$ with a sufficient As_4 flux (a), a large amount of incident $(CH_3)_3Ga$ decomposed to gallium atoms upon releasing three methyl groups and contributing to epitaxial growth above $350^\circ C$. On the other hand, some amount of di- or mono-methyl-gallium desorbed when the substrate was exposed to $(CH_3)_3Ga$ without an As_4 flux above $350^\circ C$ (b). Below $350^\circ C$ for GaAs, as well as SiO_2 and the oxide of GaAs, incident $(CH_3)_3Ga$ molecules were reflected without any decomposition both with and without an As_4 flux. Thus, the effect of the As_4 flux on the decomposition of $(CH_3)_3Ga$ was rather indirect: although a sufficient As_4 flux preserved the GaAs surface in the 2×4 arsenic-stabilized structure and the decomposition of $(CH_3)_3Ga$ was enhanced, the absence of an As_4

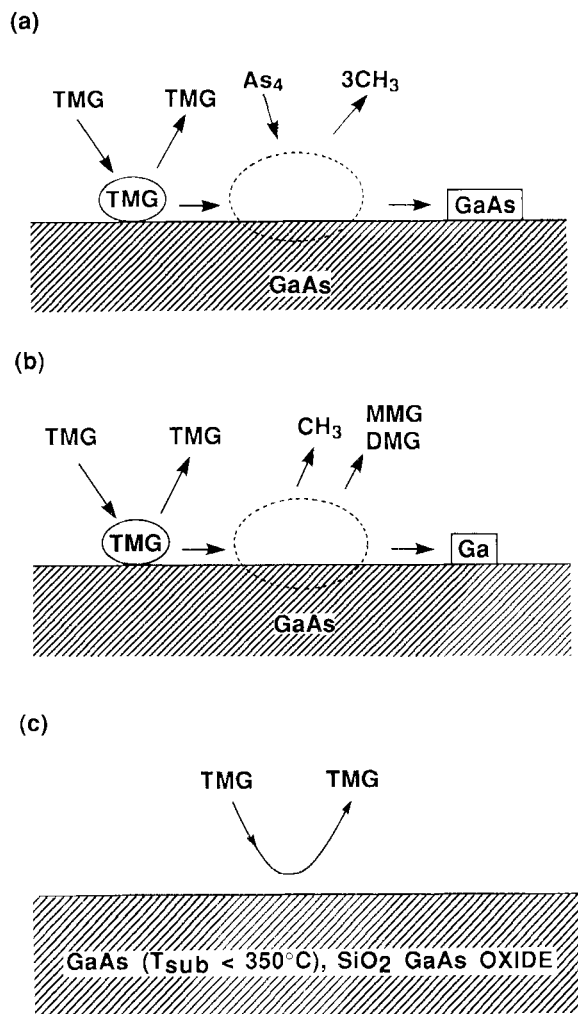


Figure 7 Decomposition pathways of $(CH_3)_3Ga$ (TMG) on GaAs: (a) above $350^\circ C$ under an As_4 flux; (b) above $350^\circ C$ in the absence of an As_4 flux; (c) below $300^\circ C$ (and on SiO_2 or on the oxidized layer of GaAs) both with and without As_4 . MMG, CH_3Ga ; DMG, $(CH_3)_2Ga$.

flux resulted in a GaAs surface with a gallium-stabilized structure; on this surface, the decomposition proceeds imperfectly and is accompanied by the desorption of either mono- or di-methyl-gallium.

Since measurements were carried out in an ultra-high vacuum with a beam-equivalent flux density of less than $5 \times 10^{-4} Pa$, the gas-phase reaction between $(CH_3)_3Ga$ and As_4 can be negligible. The decomposition of $(CH_3)_3Ga$ therefore took place on the GaAs surface, and the decomposition properties were largely dependent on the substrate surface conditions. The substrate

surface condition, such as surface reconstruction or arsenic coverage, was altered due to the exposed As_4 flux condition. As a result, the decomposition pathway of $(\text{CH}_3)_3\text{Ga}$ was also altered by the As_4 flux condition.

3.3 Decomposition of TEG on a (111)B surface

Many studies concerning MOMBE growth of GaAs on a (100) surface have been reported.¹⁹ However, papers referring to the growth on a (111) surface are rare²⁰ and, as far as we know, there has been no report concerning growth mechanism on a (111)B surface. Since the growth on a patterned surface is an interesting technique used to fabricate fine structures,²¹ the growth on a (111)-oriented surface has practical importance. In this section, results of a mass spectrometric study on the decomposition of MOs on (111)B surfaces are presented. Since the results obtained for $(\text{CH}_3)_3\text{Ga}$ and $(\text{C}_2\text{H}_5)_3\text{Ga}$ are qualitatively similar [but more prominent for $(\text{C}_2\text{H}_5)_3\text{Ga}$], we present here only the results obtained for $(\text{C}_2\text{H}_5)_3\text{Ga}$.

The measurements were performed at a substrate temperature of 420 °C. This temperature was chosen because the effects of arsenic coverage on the decomposition of $(\text{C}_2\text{H}_5)_3\text{Ga}$ could be clearly observed. Three differently reconstructed (111)B starting surfaces were examined: the 2×2 arsenic-stabilized structure, the $\sqrt{19} \times \sqrt{19}$ gallium-stabilized structure, and the 1×1 gallium saturated surface. The differences in these surface structures were due to the difference in the surface arsenic coverage.²² These surfaces could be prepared by a slightly different procedure, as is shown in Fig. 8. At first, about 20 MLs of GaAs was grown by simultaneous supply of $(\text{CH}_3)_3\text{Ga}$ and As_4 fluxes, and annealed for 10 min in an As_4 flux at 570 °C, for each case. The 2×2 arsenic-stabilized structure was formed by this procedure. This 2×2 structure was preserved by cooling down the substrate to 420 °C in the As_4 flux. The $\sqrt{19} \times \sqrt{19}$ gallium-stabilized structure²² could be formed by closing the arsenic cell shutter immediately after annealing at 570 °C, and then cooling in a vacuum. The 1×1 structure was formed by exposing the surface to $(\text{C}_2\text{H}_5)_3\text{Ga}$ at 570 °C in the absence of an As_4 flux after annealing. It can be seen from these procedures that the 2×2 structure was the most arsenic-rich surface and that the 1×1 structure was the most gallium-rich surface.

The gallium-containing species reflected from the substrate were measured while exposing these surfaces to $(\text{C}_2\text{H}_5)_3\text{Ga}$ for 1.5 min at 420 °C in the absence of the As_4 flux. The decomposition reaction was therefore only affected by either the surface structure or arsenic coverage. Figure 9 shows the time variations of the Ga^+ signal for three differently reconstructed (111)B surfaces. Only the Ga^+ signal is shown in this figure, since the signals of the other gallium-containing species [$\text{C}_2\text{H}_5\text{Ga}^+$ and $(\text{C}_2\text{H}_5)_2\text{Ga}^+$] varied in a similar fashion. Figure 9(a) shows that a large Ga^+ signal appeared during the initial stage of $(\text{C}_2\text{H}_5)_3\text{Ga}$ exposure on the 2×2 structure (we call this a 'signal peak' in this paper), followed by a steady-state low-signal intensity. This signal peak suggests that a large amount of $(\text{C}_2\text{H}_5)_3\text{Ga}$ was reflected on the surface by the 2×2 structure. The RHEED pattern changed from the 2×2 structure to the 1×1 structure after the signal peak. In Fig. 9(b), the time variation of the Ga^+ signal also shows a signal peak during the initial stage of $(\text{C}_2\text{H}_5)_3\text{Ga}$ exposure on the $\sqrt{19} \times \sqrt{19}$ structure; the signal peak height and width, however, were smaller compared with those on the 2×2 structure. The 1×1 structure also appeared after the signal peak. On the 1×1 structure [Fig. 8(c)], the Ga^+ signal shows no signal peak, only a steady-

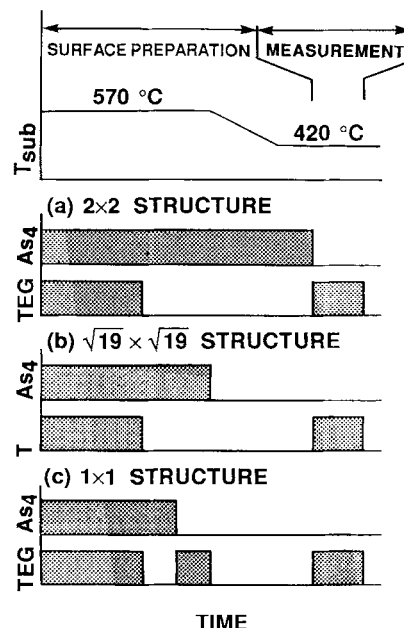


Figure 8 Preparation and measurement sequence for (111)B surfaces with the 2×2 , the $\sqrt{19} \times \sqrt{19}$, and the 1×1 structures. TEG, $(\text{C}_2\text{H}_5)_3\text{Ga}$.

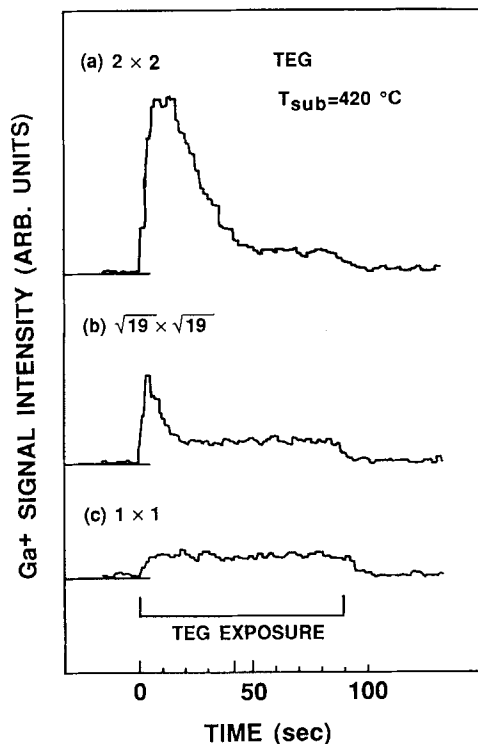


Figure 9 Time variation of the Ga^+ signal measured for three different surface structures, all at 420°C . TEG, $(\text{C}_2\text{H}_5)_3\text{Ga}$.

state signal intensity from the beginning. These characteristic features of the decomposition of $(\text{C}_2\text{H}_5)_3\text{Ga}$ were observed in the temperature range $300\text{--}550^\circ\text{C}$. Details on the temperature dependence of the intensity of the desorbed species will be presented elsewhere.²³

The result that higher arsenic coverage induces a larger signal peak suggests that a large amount of incident $(\text{C}_2\text{H}_5)_3\text{Ga}$ was reflected from the surface. In other words, the surface arsenic atoms disturb the decomposition of $(\text{C}_2\text{H}_5)_3\text{Ga}$. While a very small amount of impinged $(\text{C}_2\text{H}_5)_3\text{Ga}$ decomposes to gallium atoms, which react with surface arsenic atoms to form GaAs and to decrease arsenic coverage, the decomposition rate of $(\text{C}_2\text{H}_5)_3\text{Ga}$ increases and, finally, the surface is covered with gallium atoms and shows the 1×1 structure. The desorption of surface arsenic atoms is also considered to contribute to the decrease in arsenic coverage. Even though the microscopic mechanism for this large $(\text{C}_2\text{H}_5)_3\text{Ga}$ reflection is not clear, we suppose that the adsorbed arsenic atoms saturate dangling bonds appearing on the surface and stabilize the surface in a manner similar to the case of so-called sulfur

passivation.^{24,25} This assumption is indirectly supported by a recent STM study in which adsorbed arsenic trimer for the 2×2 structure has been proposed.²⁶ In spite of the difference in the starting surface structure, the steady-state value and resulting RHEED pattern are the same for these three cases, suggesting that the surface structure is the same when the Ga^+ signal is in the steady state. This 1×1 structure is considered to be a gallium-saturated surface, since this surface was prepared by exposing it to $(\text{C}_2\text{H}_5)_3\text{Ga}$ at 570°C at which temperature $(\text{C}_2\text{H}_5)_3\text{Ga}$ decomposed to gallium.²⁷ On this surface $(\text{C}_2\text{H}_5)_3\text{Ga}$ decomposed to gallium at 420°C in the absence of the arsenic flux.

The results presented in this section are totally different from those obtained on the (100) substrate presented before (Section 3.1), and account for the surface orientation dependence of the growth rate²⁸ as well as the absence of ALE growth on a (111)B surface.¹⁰

4 CONCLUSION

Mass spectrometry was applied to study the decomposition of trimethyl- and triethyl-gallium on substrate surfaces prepared in various ways. A cryoshrouded, apertured quadrupole mass spectrometer was used to detect gallium-containing species either desorbed or reflected from the substrate surface.

For a GaAs (100)-oriented surface, the decomposition of $(\text{CH}_3)_3\text{Ga}$ was enhanced on the 2×4 arsenic-stabilized surface, and suppressed on the gallium-stabilized surface. A similar phenomenon was also observed in measurements for $(\text{C}_2\text{H}_5)_3\text{Ga}$, though with a less-pronounced appearance. Measurements of organic species showed that $(\text{CH}_3)_3\text{Ga}$ decomposes thermally on a GaAs surface, mainly by releasing CH_3 radicals. The decomposition pathway is altered by the As_4 flux density: $(\text{CH}_3)_3\text{Ga}$ decomposes imperfectly in the absence of an As_4 flux, and desorbs mono- or di-methylgallium; it decomposes to gallium atoms under the As_4 flux and is incorporated into the epitaxially grown layer. Atomic layer epitaxy, in which $(\text{CH}_3)_3\text{Ga}$ and an arsenic source are supplied alternately, involves the desorption of alkyl-gallium with fewer than three methyl groups.

For a (111)B surface, the decomposition of $(\text{CH}_3)_3\text{Ga}$ and $(\text{C}_2\text{H}_5)_3\text{Ga}$ was suppressed by surface arsenic coverage, and was rather enhanced

on the gallium-saturated surface. This is totally different from the case of the (100) surface. This result accounts for the reported orientation dependence of the growth rate; the growth rate on a (100) surface is larger than that on a (111)B surface under a large V/III condition.

The results presented in this paper show that the arsenic atoms on the substrate surface and/or surface arsenic coverage affect largely the decomposition rate and its mechanism of both $(\text{C}_2\text{H}_5)_3\text{Ga}$ and $(\text{CH}_3)_3\text{Ga}$. Moreover, this effect is rather complicated: the surface arsenic coverage enhances the thermal decomposition of $(\text{C}_2\text{H}_5)_3\text{Ga}$ and $(\text{CH}_3)_3\text{Ga}$ on a GaAs (100) surface, but suppresses it on a (111)B surface. The surface arsenic coverage could be changed by the arsenic flux conditions and surface temperature. These results can be applied to the fabrication of fine structures.

Acknowledgements The authors would like to thank Dr Isu and Mr Watanabe for helpful discussions concerning the growth mechanism of MOMBE. They also thank Dr Y Katayama and Dr I Hayashi for their helpful discussions and continuous encouragement.

REFERENCES

1. Esaki, L and Tsu, R *IBM Research Note*, RC-2418, 1969
2. Arakawa, Y, Sakaki, H, Nishioka, M and Miura, N *IEEE J. Quantum Electron.*, 1983, QE-18: 10
3. Tokumitsu, E, Kudou, Y, Kongai, M and Takahashi, K *J. Appl. Phys.*, 1984, 55: 3163
4. Ohki, Y, Hiratani, Y and Yamada, M *Jpn. J. Appl. Phys.*, 1989, 28: L1486
5. Ohki, Y and Hiratani, Y *J. Cryst. Growth*, 1990, 105: 77
6. Hiratani, Y, Ohki, Y, Sugimoto, Y, Akita, K, Taneya, M and Hidaka, H *Jpn. J. Appl. Phys.*, 1990, 29: L1360
7. Ranke, Y and Jacobi, K *Prog. Surf. Sci.*, 1981, 10: 1
8. Cho, A Y *J. Appl. Phys.*, 1971, 42: 2074
9. Pashley, M D, Haberen, K W and Gaines, J M *Appl. Phys. Lett.*, 1991, 58: 406; Tanaka, I and Ohkouchi, S, private communication
10. Nishizawa, J, Kurabayashi, T, Abe, H and Sakurai, N *J. Electrochem. Soc.*, 1987, 134: 945
11. Gibson, E M, Foxon, C T, Zhang, J and Joyce, B A *J. Cryst. Growth*, 1990, 105: 81
12. Chiu, T H, Cunningham, J E, Robertson, A and Malm, D L *J. Cryst. Growth*, 1990, 105: 155
13. Ohki, Y and Hiratani, Y *Jpn. J. Appl. Phys.*, 1990, 29: L1036
14. Ohki, Y and Hiratani, Y *Extended Abstracts of the 22nd Conference on Solid State Devices and Materials, Sendai*, 1990, pp 485-488
15. Tu, C W, Liang, B W and Chin, T P *J. Cryst. Growth*, 1990, 105: 195
16. Isu, T, Hata, M and Watanabe, A, *J. Cryst. Growth*, 1990, 105: 209
17. Memmert, U, Yu, M L and Kuech, T F Private communication 1989
18. Creighton, J R *Surf. Sci.*, 1990, 234: 287
19. For example, papers in *J. Cryst. Growth*, 1990, 105
20. Konagai, M, Yamada, T, Akatsuka, T, Nozaki, S, Miyake, R, Saito, K, Fukamachi, T, Tokumitsu, E and Takahashi, K *J. Cryst. Growth*, 1990, 105: 359
21. Dzurko, K M, Hummell, S G, Menu, E P and Dapkus, P D *J. Electron. Mater.*, 1990, 19: 1367
22. Cho, A Y *J. Appl. Phys.*, 1970, 41: 2780
23. Ohki, Y, Hiratani, Y and Sasaki, M *J. Cryst. Growth* (to be published)
24. Sandroff, C J, Nottenburg, R N, Bischoff, J C and Baht, R *Appl. Phys. Lett.*, 1987, 51: 33
25. Hirayama, H, Matsumoto, Y, Oigawa, H and Nannichi, Y *Appl. Phys. Lett.*, 1989, 54: 2565
26. Biegelson, D K, Bringans, R D, Northrup, J E and Swartz, L E *Phys. Rev. Lett.*, 1990, 65: 452
27. Kobayashi, N, Benchimol, J L, Alexander, F and Gao, Y *Appl. Phys. Lett.*, 1987, 51: 1907
28. Yamaguchi, K and Okamoto, K *J. Cryst. Growth*, 1989, 94: 203